Confinement-induced instability of thin elastic film

A. Ghatak
Department of Chemical Engineering, Indian Institute of Technology, Kanpur 208016, India
(Received 22 October 2005; published 6 April 2006)

A confined incompressible elastic film does not deform uniformly when subjected to adhesive interfacial stresses but with undulations which have a characteristic wavelength scaling linearly with the thickness of the film. In the classical peel geometry, undulations appear along the contact line below a critical film thickness or below a critical curvature of the plate. Perturbation analysis of the stress equilibrium equations shows that for a critically confined film the total excess energy indeed attains a minimum for a finite amplitude of the perturbations which grow with further increase in the confinement.

DOI: 10.1103/PhysRevE.73.041601 PACS number(s): 68.35.Np, 68.35.Gy

I. INTRODUCTION

The spontaneous surface and interfacial instabilities of thin liquid films have been studied in different contexts—e.g., the classical Saffman-Taylor [1] problem in a Hele Shaw cell in which flow-driven fingering patterns develop at the moving interface of two viscous or viscoelastic liquids [2,3], disjoining pressure-induced rupturing and dewetting [4,5] of ultrathin viscous films, spiral instabilities in viscometric flow of a viscoelastic liquid [6,7], and fingering instability and cavitation during the peeling of a layer of viscoelastic adhesive [8,9]. While most of these viscous and viscoelastic systems have been well characterized experimentally and theoretically, similar surface undulations of confined thin elastic films pose a different kind of problem despite geometric commonalities with many of the liquid systems, the essential difference being that unlike in the liquid system there is no flow of mass and consequent permanent deformation in the elastic body, where the extent of deformation is governed by the equilibrium of the external surface or body forces on the material and the elastic forces developed.

The specific system that will be described in this paper is a thin layer of elastic adhesive confined between a rigid and a flexible plate. While the film remains strongly bonded to the rigid substrate, the flexible plate is detached from it in the classical peel geometry. A high aspect ratio of such systems is noteworthy as the lateral length scale far exceeds the thickness of the film, resulting in high degree of confinement for the adhesive. As a result, adhesive stresses at the interface do not always result in a uniform deformation throughout the whole area of contact; rather, spatially varying deformations [10–13] attain lower energy for the system. Experimentally we see the existence of a critical thickness of the film or a critical curvature of the flexible plate below which the contact line between the film and flexible plate does not remain straight, but turns undulatory with a characteristic wavelength which increases linearly with the thickness of the film [14]. While experimentally this phenomenon has been characterized, there is not much understanding as to what drives this instability in a nonflow purely elastic system and how the curvature of the plate or the thickness of the film results in a critical confinement of the film. Here I present a perturbation analysis which addresses these questions, highlighting the dual effects of the incompressibility of the elastic film and its confinement.

II. PROBLEM FORMULATION

The schematic of our experiment is represented in Fig. 1(a) in which an elastic film of thickness h and shear modulus μ remains strongly bonded to a rigid substrate while a flexible plate of rigidity D in contact with the film in the form of a curved elastica is supported at one end using a spacer of height Δ. The straight contact line between the film and plate becomes wavy when the film thickness h decreases below a critical value h_c or the curvature of the plate decreases below a critical value $1/\rho_c$. Figure 1(b) represents a typical video micrograph of such undulations which are characterized by two different length scales: the separation distance λ between the waves which scales as $\lambda \sim 4\,h$ and the amplitude A which varies with D and μ as $A \sim (D/\mu)^{1/3}$ [14]. The figure depicts also the coordinate system in which x, y, and z axes represent, respectively, the direction of propagation of the contact line, the direction of the wave vector, and the thickness coordinate of the film. The y axis is located along the tips of the waves so that the film is completely out of contact with the plate at $0 < x < a$. Assuming the adhesive film to be incompressible and purely elastic with no viscous effect, we write the following stress equilibrium relations in the absence of any body force:

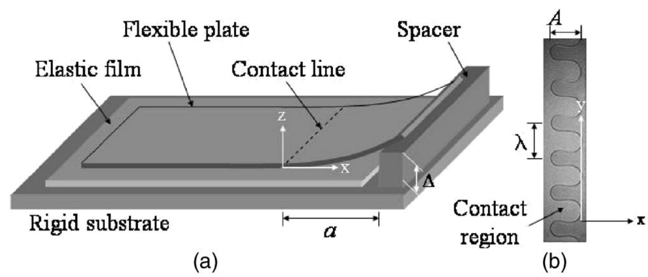

FIG. 1. (a) Schematic of the experiment in which a model elastic adhesive remains bonded to a rigid substrate and a flexible plate is detached from it with the help of a spacer inserted at the opening of the crack. For a critically confined film, the contact line does not remain smooth but becomes undulatory as shown in video micrograph (b).

1539-3755/2006/73(4)/041601(7)/$23.00

$$p_x = \mu(u_{xx} + u_{yy} + u_{zz}),$$

$$p_y = \mu(v_{xx} + v_{yy} + v_{zz}),$$

$$p_z = \mu(w_{xx} + w_{yy} + w_{zz}), \quad (1)$$

where u, v, and w are the displacements in the x, y, and z directions, respectively, and p is the pressure. Here and everywhere, $s_x=\partial s/\partial x$ and $s_{xx}=\partial^2 s/\partial x^2$. The incompressibility of the film results in

$$u_x + v_y + w_z = 0. \quad (2)$$

These equations are solved using the following set of boundary conditions (BC's): (a) Since the film remains strongly bonded to the substrate, we use the no-slip boundary condition at the interface of the film and substrate ($z=0$),

$$u(z=0) = v(z=0) = w(z=0) = 0. \quad (3)$$

(b) We assume frictionless contact at the interface of the film and cover plate, $z=h$, which results in zero shear stress at the interface,

$$\sigma_{xz}(x,y,h) = 0 = \sigma_{yz}(x,y,h). \quad (4)$$

(c) We assume continuity of normal stress across the interface ($z=h$) which implies that the normal stress on the film is equal to the bending stress on the plate,

$$\sigma_{zz}(z=h) = -D\nabla^2\psi(z=h) \quad \text{at } x<0; \quad (5)$$

here, $\nabla \equiv \partial^2/\partial x^2 + \partial^2/\partial y^2$ is the two-dimensional Laplacian, D is the flexural rigidity of the plate, and $\psi = w|_{x,z=h}$ is its vertical displacement. Since the plate bends only in the direction of the x coordinate, its vertical displacement ψ remains uniform along the y axis; hence, we simplify BC (5) as

$$\sigma_{zz}(z=h) = -D\psi_{xxxx}(z=h) \quad \text{at } x<0. \quad (6)$$

At $0<x<a$ there is no traction either on the film or plate which yields

$$\sigma_{xz}|_{z=h} = \sigma_{yz}|_{z=h} = \sigma_{zz}|_{z=h} = 0. \quad (7)$$

Equations (1) and (2) can be written in dimensionless form using the following dimensionless quantities:

$$X = xq, \quad Y = y/h, \quad Z = z/h, \quad U = uq, \quad V = v/h,$$

$$W = w/h, \quad \Psi = \psi/h, \quad P = p\epsilon^2/\mu.$$

While the thickness h of the film is the characteristic length along the y and z axes, q^{-1} is that along x. The length q^{-1} can be derived as the ratio of the deformability of the plate and film [15,16]: $q^{-1}=(Dh^3/3\mu)^{1/6}$. The quantity $\epsilon=hq$ defined as the ratio of the two characteristic lengths is a measure of the confinement of the film such that a lower value of ϵ represents a more confined film. Equations (1) and (2) can then be written in the following dimensionless form:

$$P_X = \epsilon^2 U_{XX} + U_{YY} + U_{ZZ},$$

$$P_Y = \epsilon^4 V_{XX} + \epsilon^2(V_{YY} + V_{ZZ}),$$

$$P_Z = \epsilon^4 W_{XX} + \epsilon^2(W_{YY} + W_{ZZ}),$$

$$0 = U_X + V_Y + W_Z, \quad (8)$$

while the boundary conditions (3)–(7) result:

$$\begin{aligned}
&(a) \quad U(Z=0) = V(Z=0) = W(Z=0) = 0,\\
&(b) \quad \sigma_{XZ}(X,Y,Z=1) = 0 = \sigma_{YZ}(X,Y,Z=1),\\
&(c) \quad -P(Z=1) + 2\epsilon^2 W_Z(Z=1) = -3\Psi_{XXXX} \quad \text{at } X<0,\\
&(d) \quad 0 = \Psi_{XXXX} \quad \text{at } 0<X<aq,
\end{aligned} \quad (9)$$

where aq is the dimensionless crack length. Equation (8) is solved by the regular perturbation technique which assumes that the solutions consist of two components: the base solutions which remain uniform along the Y coordinate and the correction term which incorporates the spatial variation along the Y axis. Thus the base solutions are of order ϵ^0 and the perturbed solutions are of order $\epsilon^2, \epsilon^4, \ldots$, so that any variable $T(X,Y,Z)=T_0(X,Z)+\epsilon^2 T_1(X,Y,Z)+\epsilon^4 T_2(X,Y,Z)+\cdots$ where $T=P$, U, V, and W. Inserting these definitions into Eq. (8) and separating the base (Y independent) and perturbed terms yields

$$P_{0X} = (\epsilon^2 U_{0XX} + U_{0ZZ}), \quad P_{0Z} = (\epsilon^4 W_{0XX} + \epsilon^2 W_{0ZZ}),$$

$$0 = U_{0X} + W_{0Z}, \quad (10)$$

which are solved using the BC's

$$\begin{aligned}
&(a) \quad U_0|_{Z=0} = W_0|_{Z=0} = 0,\\
&(b) \quad U_{0Z}|_{Z=1} + \epsilon^2 W_{0X}|_{Z=1} = 0,\\
&(c) \quad -P_0|_{Z=1} + 2\epsilon^2 W_{0Z}|_{Z=1} = -3\Psi_{0XXXX} \quad \text{at } X<0,\\
&(d) \quad 0 = \Psi_{0XXXX} \quad \text{at } 0<X<aq
\end{aligned} \quad (11)$$

and

$$\epsilon^2 P_{1X} + \epsilon^4 P_{2X} = \epsilon^2(U_{1YY} + U_{1ZZ}) + \epsilon^4(U_{1XX} + U_{2YY} + U_{2ZZ}) + \epsilon^6 U_{2XX},$$

$$\epsilon^2 P_{1Y} + \epsilon^4 P_{2Y} = \epsilon^4(V_{1YY} + V_{1ZZ}) + \epsilon^6(V_{1XX} + V_{2YY} + V_{2ZZ}),$$

$$\epsilon^2 P_{1Z} + \epsilon^4 P_{2Z} = \epsilon^4(W_{1YY} + W_{1ZZ}) + \epsilon^6(W_{1XX} + W_{2YY} + W_{2ZZ}),$$

$$0 = U_{1X} + V_{1Y} + W_{1Z}, \quad (12)$$

which are solved using

$$\begin{aligned}
&(a) \quad U_1|_{Z=0} = V_1|_{Z=0} = W_1|_{Z=0} = U_2|_{Z=0} = 0,\\
&(b) \quad \epsilon^2 U_{1Z}|_{Z=1} + \epsilon^4(W_{1X} + U_{2z})|_{Z=1} = 0 = \epsilon^2(V_{1Z} + W_{1Y})|_{Z=1},\\
&(c) \quad P_1|_{Z=1} = 3\Psi_{1XXXX} \quad \text{at } X<0,\\
&(d) \quad 0 = \Psi_{1XXXX} \quad \text{at } 0<X<aq.
\end{aligned} \quad (13)$$

Base solution. Since for a thin film $\epsilon^2 \ll 1$, Eqs. (10) and (11) can be simplified by neglecting the terms containing ϵ^2. Integration of the resulting equations (presented in detail in Ref. [16]) finally leads to the following solution for the base components of the displacements in the film and plate:

$$U_0 = (3Z^2/2 - 3Z)F'\phi_1(X), \quad W_0 = (3Z^2/2 - Z^3/2)F'\phi_2(X),$$

$$\phi_1 = e^{X/2}[aqe^{X/2} + (3aq+4)\sin(\sqrt{3}X/2)/\sqrt{3} - aq\cos(\sqrt{3}X/2)],$$

$$\phi_2 = e^{X/2}[aqe^{X/2} + (3aq+2)\sin(\sqrt{3}X/2)/\sqrt{3} + (aq+2)\cos(\sqrt{3}X/2)],$$

$$F' = 3\bar{\Delta}/[6 + 12aq + 9(aq)^2 + 2(aq)^3], \quad \bar{\Delta} = \Delta/h,$$

$$\Psi_0 = F'\phi_2(X) \quad (X<0)$$
$$= F'[2(aq+1) + (3aq+2)X + aqX^2 - X^3/3] \quad (0<X<aq), \tag{14}$$

which suggest oscillatory variation along X with wavelength ~ 5, implying that the relevant length scale along x is $\sim 5q^{-1}$. The displacement profiles in Eqs. (14) can be used to obtain the following expression for the dimensionless work of adhesion [16] $G = W_A/(\mu/q)$:

$$G = g(aq)[27\bar{\Delta}^2/2\epsilon(aq)^4],$$

$$g(aq) = 8(aq)^4[12 + 46(aq) + 72(aq)^2 + 56(aq)^3 + 21(aq)^4 + 3(aq)^5]/3[6 + 12(aq) + 9(aq)^2 + 2(aq)^3]^3, \tag{15}$$

in which $g(aq)$ is the correction to the classical result of Obreimoff [17] for peeling off a rigid substrate.

Perturbation analysis. Matching the coefficients for ϵ^i, $i=2,4$, on the left- and right-hand sides of Eqs. (12) results in the following set of equations:

$$\epsilon^2: \quad P_{1X} = U_{1YY} + U_{1ZZ}, \quad P_{1Y} = 0, \quad P_{1Z} = 0,$$

$$\epsilon^4: \quad P_{2X} = U_{1XX} + U_{2YY} + U_{2ZZ}, \quad P_{2Y} = V_{1YY} + V_{1ZZ},$$

$$P_{2Z} = W_{1YY} + W_{1ZZ},$$

$$U_{1X} + V_{1Y} + W_{1Z} = 0. \tag{16}$$

We assume also that the excess quantities vary sinusoidally along the Y axis, so that $T_i = \bar{T}_i\sin(KY)$; $T = U, W, P$; $V_i = \bar{V}_i\cos(KY)$, $i=1,2$; $K = 2\pi/(\lambda/h)$ is the dimensionless wave number of the perturbed waves. Equations (16) are solved using the following boundary conditions derived from Eqs. (13):

$$\text{(a) at } Z=0, \quad \bar{U}_1 = \bar{V}_1 = \bar{W}_1 = \bar{U}_2 = 0,$$

$$\text{(b) at } Z=1, \quad \bar{U}_{1Z} = 0, \quad (\bar{U}_{2Z} + \bar{W}_{1X}) = 0,$$

$$(\bar{V}_{1Z} + \bar{W}_{1Y}) = 0,$$

$$\text{(c) at } Z=1, \quad X<0, \quad \bar{P}_1 = 3\Psi_{1XXXX}, \tag{17}$$

$$\text{at } 0<X<aq \;\; 0 = \Psi_{1XXXX},$$

where $\Psi_1 = \bar{W}_1(X, Z=1)$ is the vertical displacement of the flexible plate at $Z=1$. The assumption of a sinusoidal dependence on Y is a simplification which is apparent from the video micrographs of the contact line as in Fig. 1(b) which show that the film and plate remain in contact whole through the area of the finger, implying that the deformation of the film is not perfectly sinusoidal, as it would mean a line contact between the plate and film. However, here I assume a sinusoidal variation to keep the calculations simple. Since the plate does not bend in the direction of Y, Ψ_1 and Ψ_{1XXXX} both remain uniform along this axis; consequently, in BC (17)(c), the bending stress on the plate is equated to $\bar{P}_1$. Equations (16) suggest that P_1 remains independent of Y and Z although U_1 varies along Y; hence, the only solution for P_1 that can satisfy Eqs. (16) is $P_1 = 0$. Other components of the excess displacements are obtained as

$$U_1 = 0,$$

$$V_1 = \frac{C(X)}{K}\left[\left(\frac{-2K(e^K + e^{-K})}{e^K + e^{-K} + 2Ke^K}\right)\sinh(KZ) + KZ\left(\frac{e^K + e^{-K} - 2Ke^{-K}}{e^K + e^{-K} + 2Ke^K}e^{KZ} - e^{-KZ}\right)\right]\cos(KY),$$

$$W_1 = \frac{C(X)}{K}\left[-\frac{2e^K + 2e^{-K} + 2K(e^K - e^{-K})}{e^K + e^{-K} + 2Ke^K}\sinh(KZ) + KZ\left(\frac{e^K + e^{-K} - 2Ke^{-K}}{e^K + e^{-K} + 2Ke^K}e^{KZ} + e^{-KZ}\right)\right]\sin(KY). \tag{18}$$

Here, only the lowest-order terms in ϵ are computed since the higher-order terms enhance the accuracy insignificantly. Since for all our experiments $\epsilon < 0.3$, the above solutions imply that the excess deformations in the film occur under very small excess pressure which is of the order of $\epsilon^4 < 0.01$. This excess pressure, however small, varies along Y, implying that it should depend upon the distance between the plate and film. Nevertheless, the excess traction which results from the distance-dependent forces [18,19] applies only in the immediate vicinity (<0.1 μm) of the contact between the film and plate as the gap between the two increases rather sharply [could be observed in atomic force microscopy (AFM) images of the permanent patterns of surface undulations]. Hence, it does not contribute any significantly to the overall energetics.

While Eq. (18) elaborates the variation of excess deformations along Y and Z, their dependence on X is incorporated through the coefficient $C(X)$ which is obtained by solving Eqs. (17)(c) using the following boundary conditions:

$$\text{(i,ii)} \;\; \Psi_1|_{X=0} = C_0\Phi(K), \quad \text{(iii)} \;\; \Psi_{1X}|_{X=0-} = \Psi_{1X}|_{X=0+},$$

$$\text{(iv)} \;\; \Psi_{1XX}|_{X=0-} = \Psi_{1XX}|_{X=0+},$$

$$\text{(v,vi)} \;\; \Psi_1|_{X=-\xi} = \Psi_{1X}|_{X=-\xi} = 0,$$

$$\text{(vii,viii)} \;\; \Psi_1|_{X=aq} = \Psi_{1XX}|_{X=aq} = 0,$$

where $\xi = Aq$ is the dimensionless amplitude of the waves and $C_0\Phi(K)$ is the excess stretching of the film at $x=0$: C_0 is a constant and $\Phi(K)= \bar{W}_1/C(X)|_{X=0}=(e^{-K}-e^{3K}+4Ke^{K})/K[1+e^{2K}(1+2K)]$. (a) BC's (i), (ii), (iii), and (iv) occur because the excess displacement and slope of the plate are continuous at $X=0$; (b) at $X=-\xi$, the displacement of the plate, its slope, should vanish, which results in the BC's (v) and (vi); (c) similarly, at $X=aq$ the excess displacement and curvature of the plate is zero, which results in BC's (vii) and (viii). Incorporating these boundary conditions into the solutions of Eqs. (17)(c) yields the following expression for the excess displacement of the plate:

$$\Psi_1 = \frac{C_0\Phi(K)}{aq(3\xi+4aq)}\{-[3\xi^2+6aq\xi+2(aq)^2](X/\xi)^3 - 3(2\xi^2+3aq\xi)(X/\xi)^2 - 3[\xi^2-2(aq)^2](X/\xi) + aq(3\xi+4aq)\} \quad \text{at } X<0,$$

$$\Psi_1 = C_0\Phi(K)\left(1+\frac{aq}{\xi(3\xi+4aq)}\{(2\xi+3aq)(X/aq)^3 - 3(2\xi+3aq)(X/aq)^2 - 3[\xi^2-2(aq)^2][X/(aq)^2]\}\right) \quad \text{at } 0<X<aq. \tag{19}$$

Excess energy. The total energy of the system consists of the elastic energy of the film, bending energy of the plate, and interfacial energy:

$$\Pi = \Pi_e+\Pi_b+\Pi_i = \frac{\mu}{4}\int_{-\infty}^{0}\int_0^{2\pi/k}\int_0^h[(v_z+w_y)^2+(u_y+v_x)^2 + (u_z+w_x)^2]dzdydx + \frac{D}{2}\int_{-\infty}^{a}\int_0^{2\pi/k}(\psi_{xx})^2dydx + W_A(2\pi a/k+A_{\text{finger}}), \tag{20}$$

where A_{finger} is the interfacial area of contact at $-a<x<0$. From Eq. (20) the excess energy of the system is obtained as $\Pi_{excess}=\Pi-\Pi_0$ which is written in a dimensionless form using μ/q^3 as the characteristic energy and by substituting for variables $T=T_0+\epsilon^2T_1+\epsilon^4T_2$, where $T=U$, V, W, and P.

The expression for excess elastic energy $\mathbf{\Pi}_e$ in the film is obtained as

$$\mathbf{\Pi}_e = \frac{1}{4}\int_{-\xi}^{0}\int_0^{2\pi/K}\int_0^1\{\epsilon^6[V_{1Z}+W_{1Y}+\epsilon^2(V_{2Z}+W_{2Y})]^2 + \epsilon^8(U_{2Y}+V_{1X}+\epsilon^2V_{2X})^2+\epsilon^8[(U_{2Z}+W_{1X})+\epsilon^2W_{2X}]^2 + 2\epsilon^4(U_{0Z}+\epsilon^2W_{0X})(U_{2Z}+W_{1X}+\epsilon^2W_{2X})\}dZdYdX, \tag{21}$$

where the excess energy is estimated within a distance $-\xi \leqslant X \leqslant 0$. Considering only the leading-order terms (ϵ^4 and ϵ^6) expression (21) simplifies to

$$\mathbf{\Pi}_e = \frac{\epsilon^6}{4}\int_{-\infty}^{0}\int_0^{2\pi/K}\int_0^1(V_{1Z}+W_{1Y})^2dZdYdX. \tag{22}$$

Substituting the expressions for V_1 and W_1 from Eqs. (18) into Eq. (22) yields

$$\mathbf{\Pi}_e = \epsilon^6{C_0}^2f_2(\xi,aq,K)/4 = \epsilon^6{C_0}^2f_0(K)\bar{f}_2(\xi,aq)/4. \tag{23}$$

Similarly, the dimensionless excess bending energy $\mathbf{\Pi}_b$ of the plate is obtained as

$$\mathbf{\Pi}_b = (3\pi/K)\int_{-xi}^{aq}[2\epsilon^2\Psi_{0XX}\Psi_{1XX}+\epsilon^4(\Psi_{1XX}+\epsilon^2\Psi_{2XX})^2]dX. \tag{24}$$

Considering only the leading-order terms ϵ^2 and ϵ^4, Eq. (24) simplifies to

$$\mathbf{\Pi}_b = \frac{3\pi}{K}\int_{-xi}^{aq}(2\epsilon^2\Psi_{0XX}\Psi_{1XX}+\epsilon^4\Psi_{1XX}^2)dX. \tag{25}$$

Substituting the expressions for Ψ_0 and Ψ_1 from Eqs. (14) and (19), $\mathbf{\Pi}_b$ is obtained as

$$\mathbf{\Pi}_b = \epsilon^2C_0\bar{\Delta}f_3(\xi,aq,K)+\epsilon^4{C_0}^2f_1(\xi,aq,K). \tag{26}$$

The interfacial energy is estimated as

$$\mathbf{\Pi}_i = 2G\epsilon\int_0^{\pi/K}\frac{\xi}{2}\sin(KY)dY = \frac{2G\xi\epsilon}{K}. \tag{27}$$

Substituting the expression for G from Eqs. (15) into Eq. (27) and combining all the three energies yields the total excess energy as

$$\mathbf{\Pi} = [\epsilon^6f_2(\xi,aq,K)+\epsilon^4f_1(\xi,aq,K)]{C_0}^2+\epsilon^2f_3(\xi,aq,K)\bar{\Delta}C_0 + \frac{27\bar{\Delta}^2\xi}{K}\frac{g(aq)}{(aq)^4}. \tag{28}$$

The expressions for $f_1(\xi,aq,K)$, $f_2(\xi,aq,K)$, and $f_3(\xi,aq,K)$ are obtained using Mathematica and are not being presented here since they could not be written in a compact form.

III. RESULTS AND DISCUSSION

The expression for excess energy in Eq. (28) accounts for the combined effects of three sets of parameters; ϵ, the confinement parameter; ξ and K, the characteristic length scale of the perturbations; and aq and $\bar{\Delta}$, the length scale of the geometry of the experiment. In what follows, we look for solutions of these different sets of parameters which result in negative excess energy associated with the instability.

While it is evident from Eq. (28) that ξ and K are nonlinearly coupled quantities, the physics of the problem is better understood if we study their effects separately. We do that following the observation that the excess displacements in the film but not that of the plate are functions of Y, which allows us to assume that the dimensionless wave number K of the perturbations is determined solely by the minima of the excess elastic energy $\mathbf{\Pi}_e$ and not the other components of the total excess energy. Although this assumption is not exactly correct as the displacement Ψ of the plate is also a function of K, experimental observation that the amplitude remains nearly independent of the wavelength [14] suggests that the above assumption should not insert much inaccuracy into the calculation.

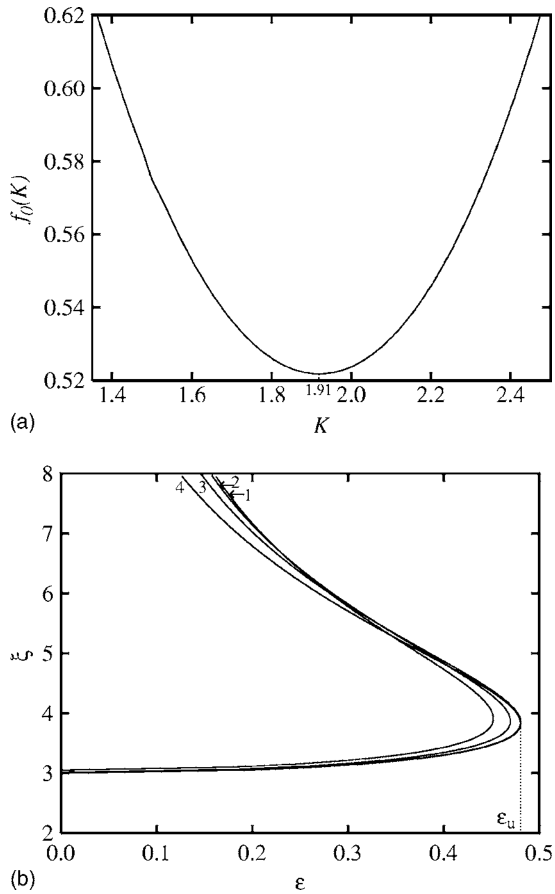

FIG. 2. (a) Dimensionless elastic energy of the film is plotted against the dimensionless wave number K of the surface undulations. The energy of the film attains a minimum at $K=1.91$ implying that the wavelength varies with thickness of the film as $\lambda=3.3h$. (b) Amplitude ξ is plotted against the limiting values of ϵ from Eq. (30) for different values of the dimensionless length aq. Curves 1–4 represent $aq=5$, 15, 25, and 55, respectively. $\epsilon_u=0.48$ is the upper limit for ϵ beyond which no real solution for C_0 exists.

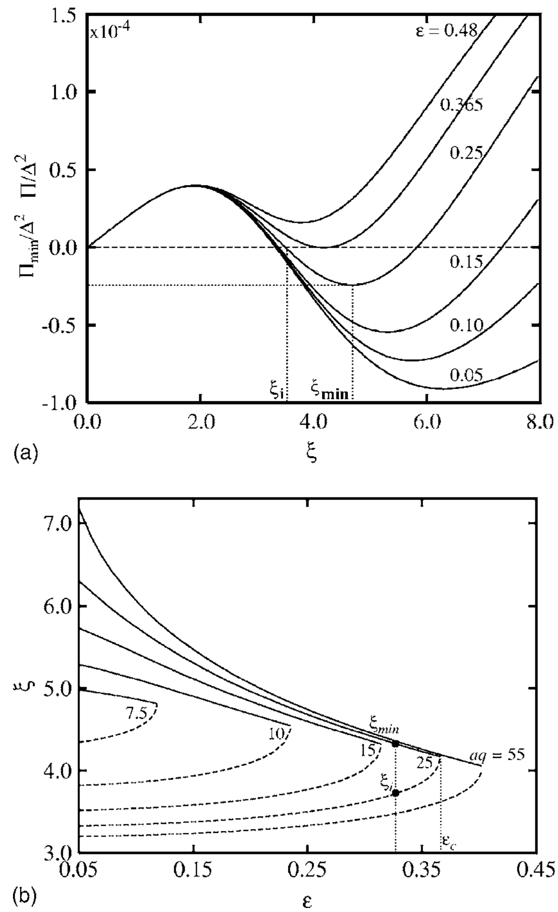

FIG. 3. (a) Dimensionless excess energy is plotted against the dimensionless amplitude of the waves for different values of the confinement parameter ϵ. The curves are obtained using representative values for the dimensionless parameters: $aq=25$, and $K=1.91$. (b) Bifurcation diagram showing variation of ξ w.r.t. ϵ for different values of aq and $K=1.91$. The dotted and the solid lines represent respectively ξ_i vs ϵ and $\xi_{\min}$ vs ϵ. No solution for ξ exists beyond ϵ_c.

The plot of excess elastic energy $\mathbf{\Pi}_e$ vs the wave number K in Fig. 2(a) then shows that $\mathbf{\Pi}_e$ attains a minimum when $K=1.91$. The wavelength of perturbations thus scales with the thickness of the film as $\lambda=3.3h$ which corroborates with the general observation in a wide range of experimental geometries [12–14] that λ remains independent of all the material and geometric properties of the system except h. Furthermore, the proportionality constant matches well with that observed in experiments ($\lambda=3-4h$) with rigid and flexible contacting plates.

Although the minima of $\mathbf{\Pi}_e$ occurs at $K=1.91$ irrespective of C_0 and ϵ, for both these parameters real values are desired. In fact, Eq. (28), being quadratic with respect to C_0, suggests that in the limit $\mathbf{\Pi}=0$ the real solutions for C_0 exist only when

$$[\epsilon^2 f_3(\xi,aq,K)]^2-4[\epsilon^6 f_2(\xi,aq,K)+\epsilon^4 f_1(\xi,aq,K)] \times(27\xi/K)g(aq)/(aq)^4 \geqslant 0, \tag{29}$$

resulting in the following inequality for ϵ^2:

$$\epsilon^2 \leqslant \frac{f_3{}^2(\xi,aq,K)}{4f_2(\xi,aq,K)}\frac{K}{27\xi}\frac{(aq)^4}{g(aq)}-\frac{f_1(\xi,aq,K)}{f_2(\xi,aq,K)}. \tag{30}$$

Equation (30) sets an upper bound for ϵ as evident from Fig. 2(b) where ξ and ϵ which satisfy Eq. (30) are plotted for $K=1.91$ and for different aq. When ϵ is smaller than this upper critical limit ϵ_u, two different solutions for ξ exist, the stability of which depends upon whether $\mathbf{\Pi}$ attains a minimum at these solutions. Hypothesizing that $\mathbf{\Pi}$ minimizes when $\partial\mathbf{\Pi}/\partial C_0=0$, we obtain an expression for C_0 which, when substituted in Eq. (28), yields

$$\mathbf{\Pi}=-\frac{\bar{\Delta}^2}{4}\frac{f_3(\xi,aq,K)^2}{f_1(\xi,aq,K)+\epsilon^2 f_2(K,\xi)}+\frac{27\bar{\Delta}^2\xi}{K}g(aq). \tag{31}$$

In Fig. 3(a) we plot $\mathbf{\Pi}$ from Eq. (31) with respect to ξ, for $\epsilon=0.48-0.05$. For all these cases, $\mathbf{\Pi}$ exhibits a nonmonotonic character: with an increase in ξ, it first increases until it reaches a maximum after which it decreases to attain a minimum; thereafter, it increases again. The stability of these systems is determined by the minimum of the excess energy which if positive signifies stable base solution for the contact line and unstable solution if negative. For example, for $\epsilon=0.48$, $\mathbf{\Pi}$ remains positive all through, implying that the undulation of a straight contact line would increase the total energy of the system so that a straight contact line would remain stable. On the other hand, $\epsilon=0.365$ presents a limiting case for which the minimum of the excess energy $\mathbf{\Pi}_{\min}$ attains zero and for $\epsilon=0.25$, 0.15, 0.1, and 0.05, $\mathbf{\Pi}_{\min}$ becomes negative; i.e., when the film is more than critically confined—i.e., $\epsilon<\epsilon_c=0.365$—the contact line can become unstable if sufficiently perturbed. The critical value $\epsilon_c=0.365$ thus obtained for the above set of data corroborates well with 0.3 obtained in the experiments of Fig. 1. Furthermore, a finite energy barrier at $\xi<\xi_i$ suggests that a straight contact line is not unstable for perturbations of all magnitude, because for a perturbation with amplitude $\xi<\xi_i$ the excess energy remains positive so that these perturbations decay to zero. This result too corroborates with experiment that with an increase in confinement of the film, the amplitude of the undulations never increases from exactly zero, but from a finite value. When $\xi>\xi_i$, $\mathbf{\Pi}$ decreases to become negative, so that these perturbations can grow until ξ reaches $\xi_{\min}$, at which $\mathbf{\Pi}$ attains the minimum $\mathbf{\Pi}_{\min}$; $\xi_{\min}$ is then the predicted amplitude of the undulations of the contact line.

Figure 3(b) depicts the bifurcation diagram where ξ_i (dashed line) and $\xi_{\min}$ (solid line) are plotted with respect to ϵ for variety of aq. The dashed lines signify that the perturbations whose amplitude $\xi<\xi_i$ decays to zero, whereas solid lines mean those with $\xi>\xi_i$ grow to $\xi_{\min}$. The amplitude $\xi_{\min}$ increases with increase in the confinement of the film similar to that observed in experiments, although the values predicted are somewhat (2–3 times) larger than what is observed. This discrepancy could be due to the underestimation of the excess elastic energy of the film. In Fig. 4 the combined effects of ξ and K are probed by plotting $\mathbf{\Pi}$ with respect to ξ and K. Here again $\mathbf{\Pi}_{\min}$ becomes negative for a confinement parameter ϵ below a critical value $\epsilon_c=0.365$. However, the wave number K at which the minimum occurs does not remain constant; it decreases from 2.12 to 0.5 while ϵ varies from 0.365 to 0.05. Although this prediction is somewhat different from experiments, in which ϵ varies between 0.3 and 0.1, at which K is observed to be 1.57 ± 0.1, some recent observations [20] with very thin elastic films (~0.5 μm) indeed indicate that K can decrease to 1.0 as ϵ decreases to 0.07. More experiments are clearly necessary to characterize quantitatively the effect of the coupling of the two length scales with highly confined elastic films.

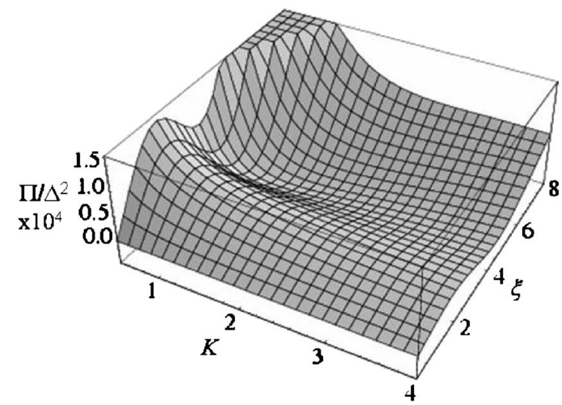

FIG. 4. Excess energy $\mathbf{\Pi}$ for $\epsilon=0.2$ and $aq=25$ is plotted with respect to amplitude ξ and wave number K.

IV. SUMMARY

The analysis shows that confinement of an incompressible elastic film leads to favorable energetics for perturbations to grow so that the film cannot deform uniformly everywhere when subjected to tensile stresses at the interface. Furthermore, the nature of the adhesion stress is not important; even the spatial variation of the surface forces plays rather an insignificant role. While the theory captures the essential physics of the problem, a slight overestimation of the amplitude possibly results from the assumption of sinusoidal variations along the Y axis which is not perfectly correct. These issues can possibly be resolved by a three-dimensional simulation of the force field near the contact line. Furthermore, it is appropriate to mention at this point that while the adhesive used in these studies was purely elastic, similar patterns should appear also with critically confined viscoelastic adhesive films. Our preliminary experiments [21] suggest that for such a situation, the instability patterns bear the signature of both the elastic instability [12,14] and viscous instability—i.e., Saffman-Taylor instability [1]. The theoretical analysis of such a system should then incorporate the dual effects of both the viscous and elastic character of the adhesive. Systematic experiments of such a system are a subject of future research.

ACKNOWLEDGMENTS

I sincerely thank Professor M. K. Chaudhury in whose laboratory at Lehigh University and under whose guidance all experiments were carried out. Many thanks to Professor L. Mahadevan, Professor Asutosh Sharma, and Professor V. Shankar for many stimulating discussions.

[1] P. G. Saffman and G. I. Taylor, Proc. R. Soc. London, Ser. A **245**, 312 (1958).
[2] G. M. Homsy, Annu. Rev. Fluid Mech. **19**, 271 (1981).
[3] J. Nittmann, G. Daccord, and H. E. Stanley, Nature (London) **314**, 141 (1985).
[4] G. Reiter, Phys. Rev. Lett. **68**, 75 (1992).
[5] A. Sharma and R. Khanna, Phys. Rev. Lett. **81**, 3463 (1998).
[6] S. J. Muller, R. G. Larson, and E. S. G. Shaqfeh, Rheol. Acta **28**, 499 (1989).
[7] G. H. McKinley, A. Öztekin, J. Byars, and R. A. Brown, J.

Fluid Mech. **285**, 123 (1995).
[8] R. J. Fields and M. F. Ashby, Philos. Mag. **33**, 33 (1976).
[9] Y. Urhama, J. Adhes. **31**, 47 (1989).
[10] A. N. Gent and P. B. Lindley, Proc. R. Soc. London, Ser. A **245**, 195 (1958).
[11] A. N. Gent and D. J. Tompkins, J. Appl. Phys. **40**, 2520 (1969).
[12] A. Ghatak, M. K. Chaudhury, V. Shenoy, and A. Sharma, Phys. Rev. Lett. **85**, 4329 (2000).
[13] W. Mönch and S. Herminghaus, Europhys. Lett. **53**, 525 (2001).
[14] A. Ghatak and M. K. Chaudhury, Langmuir **19**, 2621 (2003).
[15] D. A. Dillard, J. Appl. Mech. **56**, 382 (1989).
[16] A. Ghatak, L. Mahadevan, and M. K. Chaudhury, Langmuir **21**, 1277 (2005).
[17] J. W. Obreimoff, Proc. R. Soc. London, Ser. A **127**, 290 (1930).
[18] V. Shenoy and A. Sharma, Phys. Rev. Lett. **86**, 119 (2001).
[19] J. Sarkar, V. Shenoy, and A. Sharma, Phys. Rev. Lett. **93**, 018302 (2004).
[20] A. Sharma (personal communication).
[21] A. Ghatak, Ph.D. thesis, Lehigh University, 2003.